ISSN: 1410-8917
Jurnal Kimia Sains & Aplikasi
e-ISSN: 2597-9914

Jurnal Kimia Sains dan Aplikasi 28 (9) (2025): 529-535

Jurnal Kimia Sains dan Aplikasi
Journal of Scientific and Applied Chemistry

Journal homepage: http://ejournal.undip.ac.id/index.php/ksa

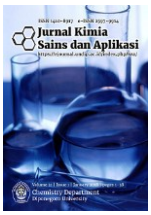

# Comparative Study on the Effect of Polyvinylpyrrolidone (PVP K30) Concentration on the Structure and Performance of Chitosan Membranes for Phosphate Ion Filtration

Retno Ariadi Lusiana [1,*], M. Ridho Shofwan Al Aziz [1], Didik Setiyo Widodo [1], Khabibi [1]

[1] Department of Chemistry, Faculty of Science and Mathematics, Diponegoro University, Semarang, Indonesia

* Corresponding author: retno.lusiana@live.undip.ac.id

https://doi.org/10.14710/jksa.28.9.529-535

Article Info

Article history:

Received: 22nd October 2025
Revised: 03rd December 2025
Accepted: 04th December 2025
Online: 08th December 2025

Keywords:
chitosan; PVP K30; porosity; filtration; phosphate ion adsorption

Abstract

The increasing concentration of phosphate in industrial and agricultural waste is a major cause of eutrophication, which threatens the balance of aquatic ecosystems. Membrane technology offers an effective approach for phosphate ion removal through the combined mechanisms of filtration and adsorption. In this study, chitosan membranes were modified with polyvinylpyrrolidone K30 (PVP K30) at four different concentrations using the phase inversion method. Increasing the PVP K30 content in the chitosan membrane enhanced water absorption, porosity, and hydrophilicity. These improvements significantly influenced phosphate ion filtration performance, resulting in a flux increase of 33–48% and an enhancement in phosphate ion rejection of 32–39% compared to the unmodified chitosan membrane. Furthermore, phosphate ion adsorption on the membrane surface was observed, which is likely attributed to the presence of surface functional groups with different charges and to membrane pore sizes comparable to the size of phosphate ions.

## 1. Introduction

The rapid growth of industrial activities has led to the discharge of large quantities of phosphate anions, which pose serious risks to the environment, human health, and aquatic ecosystems. Natural biopolymers have therefore attracted increasing attention as effective adsorbents for phosphate anions due to their biocompatibility, biodegradability, eco-friendliness, low cost, natural abundance, and ease of modification [1]. Among these materials, chitosan-based adsorbents are regarded as highly effective for removing various pollutants from industrial wastewater. The presence of active amine (– NH) and hydroxyl (–OH) groups along the chitosan backbone facilitates both physical and chemical modifications, enabling multiple adsorption mechanisms for phosphate anions.

Phosphate ions are a primary cause of eutrophication, originating from the application of fertilizers, the use of detergents, and industrial effluents. Eutrophication reduces dissolved oxygen levels and disrupts aquatic ecosystems. Various treatment methods have been employed for phosphate removal, including chemical precipitation, adsorption, and membrane filtration. Among these, membrane technology is considered efficient and environmentally friendly, as it does not require additional chemicals and allows continuous operation.

Several studies have demonstrated the effectiveness of chitosan-based materials for reducing phosphate levels in wastewater. For example, Fe(III)-modified chitosan (CS–Fe) has been reported to enhance phosphate adsorption, as Fe(III) ions release hydrogen ions under acidic conditions, increasing electrostatic attraction [2]. Karthikeyan et al. combined gelatin–$Al^{3+}$ with chitosan and observed an increased phosphate adsorption capacity due to electrostatic interactions between negatively charged phosphate ions and positively charged species ($NH_3^+$ and $Al^{3+}$) [3]. Similarly, Zhao *et al.* [4] incorporated $La^{3+}$ into chitosan, where chitosan acted as a support for $La^{3+}$ ions in phosphate binding. These findings indicate that chitosan is an active biopolymer with high potential for phosphate ion adsorption from aqueous media.

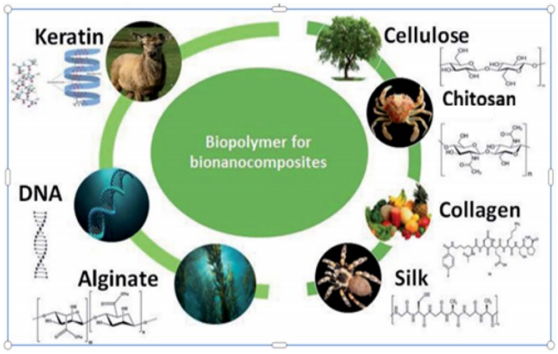


Various types of biopolymers

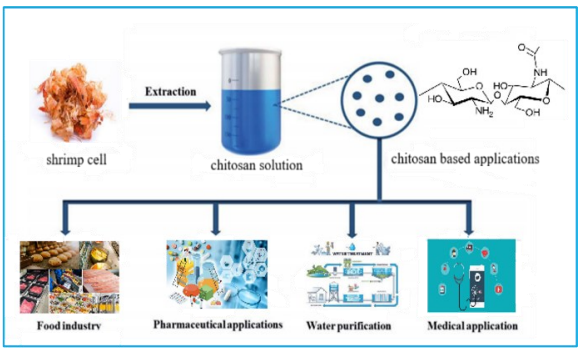


The extraction of Chitosan and its applications in diverse fields

**Figure 1**. Sources and applications of chitosan

Chitosan is a polycationic polymer owing to the presence of positively charged amino groups in its structure (pKa ≈ 6.5), which enhances its solubility in acidic and neutral solutions. Its properties are strongly influenced by factors such as molecular weight, degree of acetylation, pH, temperature, crystallinity, physical form (powder, granules, flakes, or membranes), and the presence of hydroxyl (–OH) and amino ($-NH_2$) functional groups that are readily modified through grafting or silane bonding [5]. Structurally, chitosan is similar to cellulose but contains an amino group instead of a hydroxyl group at the C-2 position, a difference that significantly broadens its application potential. Chitosan can be processed into various morphologies, including films, fibers, hydrogels, nanoparticles, and microspheres. In membrane form, chitosan functions effectively as a phosphate ion adsorbent with high adsorption capacity [6]. A membrane is defined as a thin, semipermeable layer that separates two phases and selectively allows certain species to pass through [5].

The mechanical strength and performance of chitosan membranes can be enhanced by blending with other polymers, such as polyethersulfone (PES), polyvinyl alcohol (PVA), polyvinyl chloride (PVC), polyethylene glycol (PEG), polysulfone (PSf), and polyvinylpyrrolidone (PVP). PVP K30 is a synthetic, hydrophilic, and biocompatible polymer that acts as a pore-forming agent and is widely used as a biomaterial or pharmaceutical additive [7]. The incorporation of PVP K30 into chitosan has been shown to improve membrane properties, particularly water uptake and hydrophilicity [8]. Interactions between chitosan and PVP K30 occur through hydrogen bonding between the pyrrolidone ring of PVP and the amine and hydroxyl groups of chitosan, leading to high miscibility and enhanced physicochemical properties [9]. PVP is available in various molecular weights, such as PVP K30 (≈40,000 g/mol) and PVP K90 (≈1,300,000 g/mol), and this variation significantly influences pore morphology, mechanical strength, and separation performance.

This study aims to investigate the effect of PVP K30 concentration on the performance of chitosan membranes in phosphate ion filtration, with the goal of achieving an optimal balance between flux and rejection. PVP K30 is expected to produce membranes with finer and more uniform pore structures due to its lower molecular weight, which enables homogeneous dispersion and suitable solution viscosity during membrane fabrication. Consequently, pore formation through the phase inversion process occurs more uniformly. In contrast, PVP K90, with its much higher molecular weight, markedly increases solution viscosity, leading to poorer homogeneity, larger and irregular pores, and the formation of dense regions, which can result in less stable filtration performance [9]. Therefore, this study focuses on chitosan membranes modified with PVP K30 at four different concentrations and evaluates the effectiveness of PVP K30 addition on phosphate ion filtration performance.

## 2. Experimental

### 2.1. Equipment and Materials

The materials used in this study included distilled water (Labter, UNDIP); chitosan (Chimultiguna, Cirebon, Indonesia; degree of deacetylation 87%; Mw 40,000 g/mol); polyvinylpyrrolidone K30 (PVP K30, BASF; Mw 30,000 g/mol); acetic acid (Merck; Mw 60 g/mol); ascorbic acid (Merck; Mw 176.12 g/mol); sulfuric acid (Merck; Mw 98.08 g/mol); ammonium molybdate (Merck; Mw 196.01 g/mol); sodium hydroxide (Merck; Mw 40 g/mol); sodium dihydrogen phosphate monohydrate ($NaH_2PO_4.H_2O$, Merck; Mw 137.99 g/mol); phenolphthalein (Merck; Mw 318.33 g/mol); potassium antimonyl tartrate (Merck; Mw 667.87 g/mol); methanol (Merck; Mw 32.04 g/mol); and monopotassium dihydrogen phosphate ($KH_2PO_4$, Merck; Mw 136 g/mol).

The main equipment consisted of a magnetic stirrer, casting plate, vacuum oven, homogenizer, Mitutoyo thickness meter, UV–Vis spectrophotometer (PG T-60), FTIR spectrometer (Agilent), scanning electron microscope (SEM; JEOL JSM-6510), and a low-pressure dead-end filtration system.

### 2.2. Membrane Preparation

The membranes were prepared with five different concentration variations, as listed in Table 1. A chitosan solution (1.5% w/v) was prepared by dissolving 1.5 g of chitosan in 1% (v/v) acetic acid. Separately, PVP K30 powder at the amounts specified in Table 1 was dissolved in 100 mL of distilled water. The two solutions were then

mixed at a volume ratio of 1:1 to obtain a total volume of 100 mL and stirred for 4 hours at 55°C, followed by homogenization for 15 minutes at the same temperature to ensure complete mixing. Subsequently, 10 mL of the resulting solution was poured into a Petri dish for membrane casting and dried at 50°C for 24 hours. The dried membranes were carefully removed and stored in a desiccator prior to further characterization and testing.

### 2.3. Membrane Characterization

All fabricated membranes were subjected to physicochemical characterization, including measurements of weight, density, water absorption, porosity, contact angle, biodegradability, FTIR spectroscopy to identify functional group interactions, and SEM to observe surface morphology. Measurements of weight, density, water absorption, porosity, and contact angle were performed in triplicate to minimize experimental error. Water absorption was determined using Equation (1).

$$\text{Water absorption } (\%) = \frac{W_w - W_d}{W_d} \times 100 \quad (1)$$

Where, $W_w$ is the weight of the membrane in the wet state (g), and $W_d$ is the weight of the membrane in the dry state (g).

Membrane porosity was calculated using Equation (2).

$$\text{Porosity } (\%) = \frac{(W_w - W_d)}{(\rho_w \times Ah)} \times 100 \quad (2)$$

Where, $W_w$ and $W_d$ are the wet and dry membrane weights (g), respectively; $\rho_w$ is the density of water (1 g $cm^{-3}$); $A$ is the membrane area ($cm^2$); and $h$ is the membrane thickness (cm).

Membrane hydrophilicity was evaluated through contact angle measurements using the sessile drop method.

### 2.4. Filtration Test for Phosphate Ions

Phosphate ion filtration experiments were carried out using a filtration flask connected to a vacuum pump and a Büchner funnel. A chitosan membrane (1.5%) was placed to fully cover the inner surface of the funnel. Subsequently, 1 L of a standard phosphate solution (13 ppm $NaH_2PO_4$) was poured into the funnel. Filtration was conducted in four cycles, and in each cycle, 8 mL of permeate was collected for analysis using a UV–Vis spectrophotometer at a wavelength of 875 nm. The same procedure was applied to all membrane variations. All filtration experiments were performed in triplicate.

After filtration, the used membranes were reanalyzed by FTIR spectroscopy to identify possible vibrational shifts associated with phosphate adsorption. Rejection efficiency and filtration performance were evaluated using Equations 3 to 5 [10].

$$q_e = \frac{(C_i - C_e \times V)}{m} \quad (3)$$

$$Phosphate\ removal\ (\%) = \frac{C_i - C_e}{C_i} \times 100 \quad (4)$$

$$J = \frac{V}{A \times t} \quad (5)$$

Where, $C_i$ and $C_e$ are the phosphate concentrations in the feed and permeate solutions, respectively; m is the membrane mass (g); $V$ is the volume of permeate (L); $J$ is the membrane flux (L $m^{-2}$ $h^{-1}$, LMH); $A$ is the effective membrane area ($m^2$); and $t$ is the filtration time (h).

## 3. Results and Discussion

### 3.1. FTIR Spectral Analysis

The FTIR spectra of chitosan, PVP K30, and chitosan–PVP K30 membranes with four compositional variations are presented in Figure 2. The characteristic absorption bands of chitosan include a broad band at 3432 $cm^{-1}$, attributed to the stretching vibrations of –OH and –NH groups. Bands observed at 1650 and 1587 $cm^{-1}$ correspond to amide I and –NH bending vibrations, respectively, while the band at 1080 $cm^{-1}$ is assigned to C–O–C stretching. These functional groups are consistent with those reported by Christou *et al.* [11].

The FTIR spectrum of PVP K30 exhibits a characteristic absorption band at 1289 $cm^{-1}$, corresponding to C–N stretching, which is absent in the chitosan spectrum. Absorption bands at 3391, 2952, and 1640 $cm^{-1}$ overlap with those of chitosan, indicating similar functional group regions. In addition, bands in the 1450–1500 $cm^{-1}$ range are attributed to symmetric and asymmetric C–C stretching vibrations. These spectral features are in agreement with previous findings reported by Gao *et al.* [12].

The chitosan–PVP K30 membranes exhibit distinct peaks at 1289.67 and 1289.65 $cm^{-1}$, which are associated with C–N stretching. Absorption bands at 1595.30 $cm^{-1}$ indicate –NH bending of primary amine groups, while the –OH stretching band shifts to 3415 $cm^{-1}$. This shift suggests the formation of hydrogen bonds between the –OH groups of PVP K30 and the $-NH_2$ groups of chitosan. Furthermore, absorption bands at 1647.48 and 1640.02 $cm^{-1}$ show a shift to lower wavenumbers for the C=O stretching vibration, confirming electrostatic interactions between chitosan and PVP K30. These observations are consistent with the results reported by Kumar *et al.* [13].

To further confirm the FTIR results, spectral deconvolution was performed in the wavenumber range of 3330–3260 $cm^{-1}$ to evaluate secondary amine content, as well as in the 3350–3310 $cm^{-1}$ region. The aliphatic primary amine absorption region (3330–3250 $cm^{-1}$) was also analyzed due to its potential overlap with secondary amine bands, based on reference IR spectra from Merck. The results of the deconvolution analysis of the modified chitosan membranes are shown in Figure 3.

**Table 1.** Compositional variations of chitosan–PVP K30 membranes (total casting volume: 10 mL)

| Membrane type | CS (%) | PVP K30 (%) |
|---|---|---|
| CS | 1.5 | 0 |
| CP1 | 1.5 | 0.25 |
| CP2 | 1.5 | 0.5 |
| CP3 | 1.5 | 1 |
| CP4 | 1.5 | 1.5 |

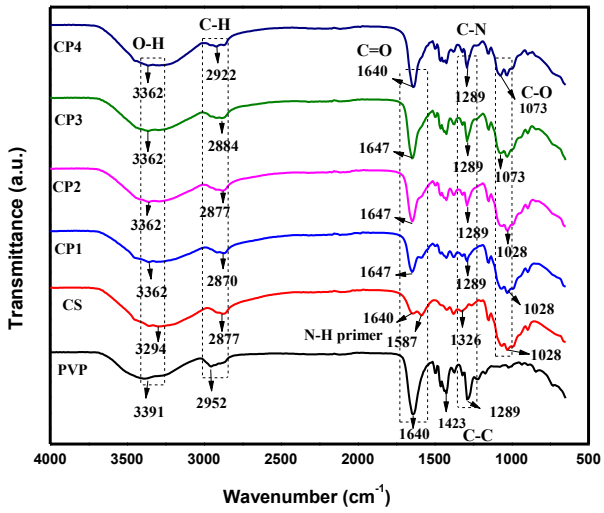


**Figure 2**. FTIR spectra of the membranes

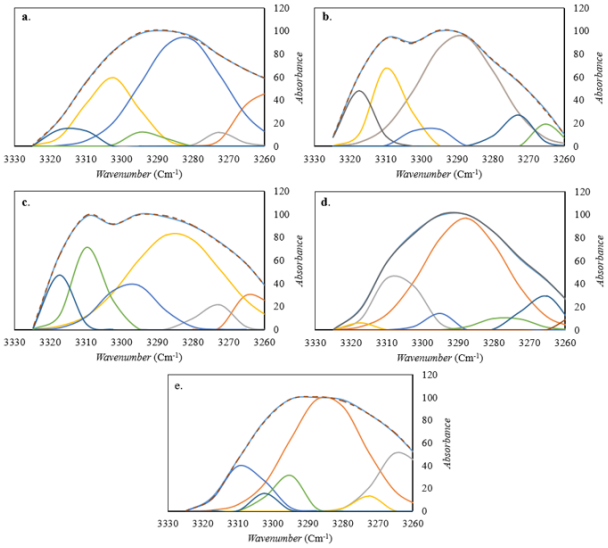


**Figure 3**. Deconvolution spectra of (a) CS, (b) CP1, (c) CP2, (d) CP3, and (e) CP4

Based on the vibrational data, the hydroxyl groups of chitosan interact with the carbonyl groups of PVP K30, leading to the formation of strong hydrogen bonds. The pyrrolidone ring in PVP K30, which contains electron-rich carbonyl groups, acts as a hydrogen bond acceptor, while chitosan provides hydroxyl and amino groups as hydrogen bond donors and co-anchoring sites. Consequently, hydrogen bonding interactions are established upon blending chitosan with PVP K30.

The deconvolution results indicate that the aliphatic primary amine group exhibits a larger peak area than the secondary amine group. This finding suggests that primary aliphatic amine groups are more abundant than secondary amine groups in both pure and modified chitosan membranes. The proposed interactions among chitosan, PVP K30, phosphate ions, and water molecules are illustrated in Figure 4.

As shown in Table 2, the modified membranes display higher –NH peak intensities compared to the unmodified chitosan membrane. This behavior is attributed to the incorporation of PVP K30, which increases the effective contribution of –NH groups, alters their chemical environment toward a more ordered configuration, and enhances the intensity of N–H vibrational modes. Consequently, after peak separation through deconvolution, the contribution of –NH groups in the modified membranes appears more pronounced than in the pristine chitosan membrane.

### 3.2. Physicochemical Properties of the Membranes

The porosity, water absorption, and hydrophilicity of the membranes are summarized in Table 3. The incorporation of PVP K30 into the chitosan matrix reduced the density of the casting solution, which consequently led to a decrease in membrane weight. Despite this reduction, the presence of PVP K30 significantly enhanced membrane porosity and water absorption. Increased porosity reflects the formation of a greater number of voids within the membrane structure, which play a crucial role in solution retention and transport during the filtration process.

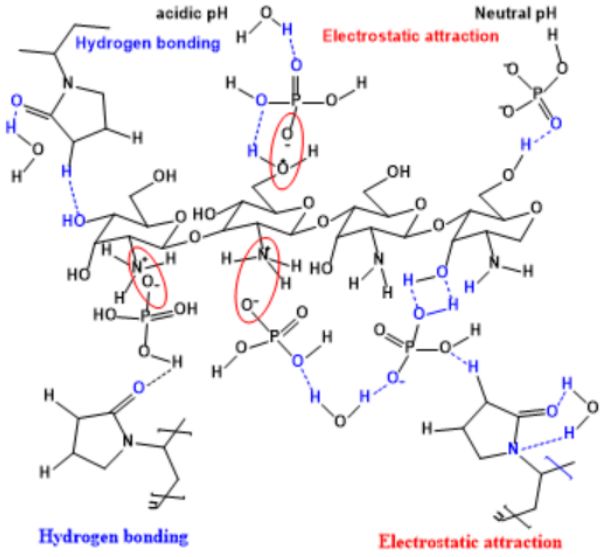


**Figure 4**. Possible orthophosphate bonding interactions in chitosan–PVP K30 and water [14]

**Table 2**. Absorbance values of the two main functional groups on the membranes

| Functional group | CS | CP1 | CP2 | CP3 | CP4 |
|---|---|---|---|---|---|
| $-NH_2$ | 2686.27 | 2620.70 | 2665.37 | 2690.78 | 2664.98 |
| –NH– | 217.77 | 820.26 | 808.57 | 737.29 | 600.66 |

**Table 3**. Physical properties of the membranes

| Membrane type | Weight (mg) | Density (mg/mL) | Porosity (%) | Water uptake (%) | Contact angle (°) |
|---|---|---|---|---|---|
| CS | 14.10 | 1.023 | 10.91 | 90 | 84 |
| CP1 | 8.19 | 0.997 | 16.85 | 101 | 77 |
| CP2 | 8.78 | 0.997 | 23.47 | 102 | 72 |
| CP3 | 9.20 | 0.999 | 34.90 | 107 | 69 |
| CP4 | 1.80 | 1.002 | 43.34 | 110 | 54 |

PVP K30 acts as a pore-forming agent during the phase inversion process, and increasing its concentration is directly proportional to the number and size of pores generated within the membrane [15]. At relatively low concentrations, PVP K30 diffuses more uniformly within the polymer matrix, promoting more effective pore development [16].

The enhancement in water absorption is influenced not only by increased porosity but also by the intrinsic hydrophilicity of PVP K30. As a hydrophilic additive, PVP K30 interacts with water molecules through hydrogen bonding, thereby increasing the overall hydrophilicity of the membrane [15, 17, 18]. This property facilitates water uptake and induces membrane swelling. Consequently, higher PVP K30 concentrations result in greater swelling behavior due to the increased number of hydrogen bonds and enlarged free volume within the membrane structure [19].

### 3.3. Biodegradability

The biodegradation behavior of the membranes in soil is presented in Figure 5. During the first week, all membranes exhibited a decrease in weight, indicating the onset of degradation by soil microorganisms. The unmodified chitosan (CS) membrane showed a slightly slower degradation rate compared to the PVP K30–modified membranes across all concentration variations.

The incorporation of PVP K30 into the membrane matrix increased the susceptibility of the membranes to degradation. As a result, PVP K30–modified membranes degraded more rapidly than the pristine chitosan membrane, and the degradation rate increased with increasing PVP K30 concentration. This behavior is attributed to the enhanced porosity induced by PVP K30, which reduces mechanical strength and renders the membranes more vulnerable to weathering, aging, and mechanical stress within the soil environment.

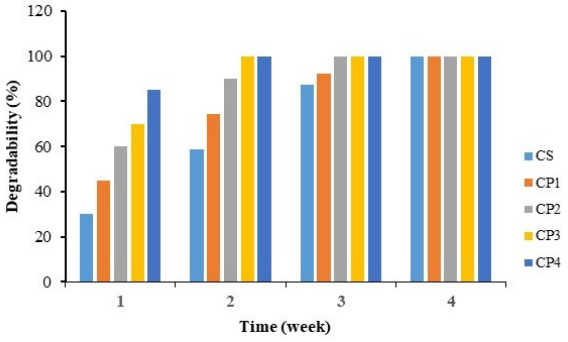


**Figure 5**. Membrane degradation over time

During the degradation, the membrane structure gradually fragmented into polymers with lower molecular weights, thereby increasing the effective surface area available for biological and chemical degradation. Moreover, the hydrophilic nature of the membranes facilitated moisture retention at the material surface, creating favorable conditions for the growth and activity of soil microorganisms. Previous studies have shown that hydrophilic additives such as PVP K30 can modify membrane morphology and accelerate biodegradation processes [15].

### 3.4. Surface Morphology

The cross-sectional morphology reveals clear differences between the pristine chitosan membrane and the PVP K30–modified membranes. As shown in Figure 6, the pure chitosan membrane exhibits a relatively smooth surface with a dense and compact structure. In contrast, the incorporation of PVP K30 results in a rougher surface and a more porous morphology, indicating the formation of a more open membrane structure with good compatibility between chitosan and PVP K30.

The formation of small pores is attributed to the high solubility of PVP K30 in the solvent system and its strong interactions with the amine groups of chitosan. This porous architecture contributes directly to the observed increase in membrane porosity, which in turn enhances water absorption capacity. Overall, these morphological changes demonstrate a strong correlation between increased porosity and improved water uptake in the chitosan–PVP K30 membranes.

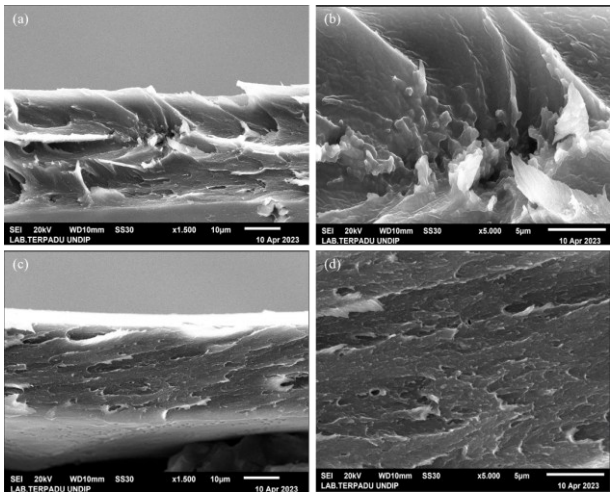


**Figure 6**. Cross-sectional SEM images of (a) CS at 1500×, (b) CS at 5000×, (c) CS–PVP K30 at 1500×, and (d) CS–PVP K30 at 5000×

### 3.5. Phosphate Filtration Performance

As shown in Figure 7, the pristine chitosan membrane exhibited an adsorption capacity of 26 mg $g^{-1}$, a flux of 20 L $m^{-2}$ $h^{-1}$, and a phosphate ion rejection efficiency of 25%. The incorporation of 0.25% PVP K30 into the chitosan membrane increased the adsorption capacity to 37 mg $g^{-1}$, the flux to 39 L $m^{-2}$ $h^{-1}$, and the phosphate rejection efficiency to 33%. These values increased progressively with increasing PVP K30 concentration. The CP4 membrane achieved the highest performance, with an adsorption capacity of 45 mg $g^{-1}$, a flux of 49 $L^{-2}$ $h^{-1}$, and a phosphate rejection efficiency of 40%. Overall, increasing the PVP K30 content in the membrane matrix enhanced phosphate rejection by approximately 30–40%, adsorption capacity by 36–44%, and flux by 36–44%. This improvement is consistent with the increase in membrane porosity and hydrophilicity, as presented in Table 3. Higher porosity provides more flow pathways, allowing a greater volume of solution to pass through the membrane and thereby increasing flux [15].

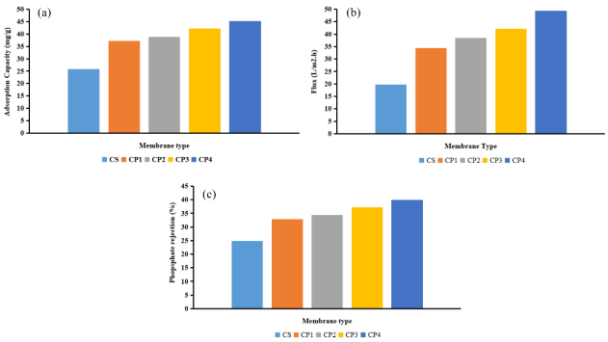


**Figure 7**. (a) Phosphate ion adsorption capacity (initial concentration: 13 mg $L^{-1}$; volume: 8 mL; time: 60 minutes; membrane dose: 92 mg), (b) membrane flux, and (c) phosphate rejection efficiency

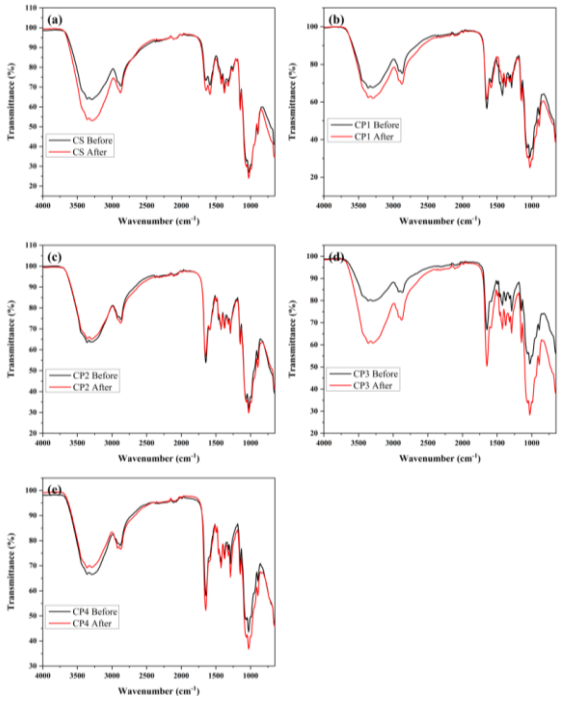


**Figure 8**. FTIR spectra before and after filtration: (a) CS, (b) CP1, (c) CP2, (d) CP3, and (e) CP4

The enhanced phosphate ion rejection observed at higher PVP K30 concentrations is likely associated with the increased number of carbonyl (C=O) groups introduced by PVP K30. These groups form hydrogen bonds with the amine and hydroxyl groups of chitosan, resulting in a more open and hydrophilic polymer network. Consequently, the number of active adsorption sites increases, additional water transport channels are created, and the positively charged chitosan surface becomes more exposed, leading to stronger electrostatic repulsion toward phosphate ions. In addition, phosphate ions passing through the membrane may also be adsorbed onto the membrane surface, potentially due to charge interactions or pore sizes comparable to the size of phosphate ions [20].

The adsorption of phosphate ions on the membrane surface was further confirmed by FTIR analysis. A comparison of the FTIR spectra before and after filtration revealed clear evidence of interactions between the adsorbate and the adsorbent. As shown in Figure 8, the used CS and CP membranes exhibited a decrease in transmittance accompanied by an increase in the absorption intensity in the 1160–1140 $cm^{-1}$ region, which corresponds to the stretching vibration of the P=O group. The increased absorbance in this region indicates that phosphate ions were bound or interacted with active functional groups on the membrane surface. This interaction is attributed to electrostatic forces between charged membrane sites and phosphate ions. Since FTIR absorbance is inversely proportional to transmittance, the enhanced P=O absorption results in lower transmittance, confirming successful phosphate capture through an adsorption mechanism.

## 4. Conclusion

The incorporation of polyvinylpyrrolidone (PVP K30) into the chitosan matrix significantly influences the membrane's structure, physicochemical properties, and phosphate filtration performance. PVP K30 functions as an effective pore-forming agent, leading to increased porosity, water uptake, and hydrophilicity of the membranes. These enhancements contribute directly to improved membrane permeability and phosphate ion filtration efficiency. Overall, the introduction of PVP K30 increased phosphate rejection by 32–61%, adsorption capacity by 44–75%, and flux by 74–150% compared to the pristine chitosan membrane.

## References

[1] Abdelazeem S. Eltaweil, Eman M. Abd El-Monaem, Hala M. Elshishini, Hisham G. El-Aqapa, Mohamed Hosny, Ahmed M. Abdelfatah, Maha S. Ahmed, Eman Nasr Hammad, Gehan M. El-Subruiti, Manal Fawzy, Ahmed M. Omer, Recent developments in alginate-based adsorbents for removing phosphate ions from wastewater: a review, *RSC Advances*, 12, 13, (2022), 8228-8248 http://doi.org/10.1039/D1RA09193J

[2] Boaiqi Zhang, Nan Chen, Chuanping Feng, Zhenya Zhang, Adsorption for phosphate by crosslinked/non-crosslinked-chitosan-Fe(III) complex sorbents: Characteristic and mechanism, *Chemical Engineering Journal*, 353, (2018), 361-372 https://doi.org/10.1016/j.cej.2018.07.092

[3] Perumal Karthikeyan, Hyder Ali Thagira Banu, Sankaran Meenakshi, Removal of phosphate and nitrate ions from aqueous solution using $La^{3+}$ incorporated chitosan biopolymeric matrix membrane, *International Journal of Biological Macromolecules*, 124, (2019), 492-504 https://doi.org/10.1016/j.ijbiomac.2018.11.127

[4] Yumeng Zhao, Lin Guo, Wei Shen, Qingda An, Zuoyi Xiao, Haisong Wang, Weijie Cai, Shangru Zhai, Zhongcheng Li, Function integrated chitosan-based beads with throughout sorption sites and inherent diffusion network for efficient phosphate removal, *Carbohydrate Polymers*, 230, (2020), 115639 https://doi.org/10.1016/j.carbpol.2019.115639

[5] Retno Ariadi Lusiana, Khabibi Khabibi, Rahmad Nuryanto, Muhammad Ridho Shofwan Al Aziz, Development and Characterization of a Chitosan and Polyvinyl Alcohol (CS/PVP)-Based Slow-Release Urea Fertilizer Membrane, *Jurnal Kimia Sains dan Aplikasi*, 27, 10, (2024), 470-476 http://doi.org/10.14710/jksa.27.10.470-476

[6] Jianlong Wang, Shuting Zhuang, Chitosan-based materials: Preparation, modification and application, *Journal of Cleaner Production*, 355, (2022), 131825 https://doi.org/10.1016/j.jclepro.2022.131825

[7] R. Poonguzhali, S. Khaleel Basha, V. Sugantha Kumari, Synthesis and characterization of chitosan/poly (vinylpyrrolidone) biocomposite for biomedical application, *Polymer Bulletin*, 74, 6, (2017), 2185-2201 http://doi.org/10.1007/s00289-016-1831-z

[8] R. H. Sizílio, J. G. Galvão, G. G. G. Trindade, L. T. S. Pina, L. N. Andrade, J. K. M. C. Gonsalves, A. A. M. Lira, M. V. Chaud, T. F. R. Alves, M. L. P. M. Arguelho, R. S. Nunes, Chitosan/pvp-based mucoadhesive membranes as a promising delivery system of betamethasone-17-valerate for aphthous stomatitis, *Carbohydrate Polymers*, 190, (2018), 339-345 https://doi.org/10.1016/j.carbpol.2018.02.079

[9] Katarzyna Lewandowska, Miscibility and interactions in chitosan acetate/poly(N-vinylpyrrolidone) blends, *Thermochimica Acta*, 517, 1, (2011), 90-97 https://doi.org/10.1016/j.tca.2011.01.036

[10] Hyder Ali Thagira Banu, Perumal Karthikeyan, Sivakumar Vigneshwaran, Sankaran Meenakshi, Adsorptive performance of lanthanum encapsulated biopolymer chitosan-kaolin clay hybrid composite for the recovery of nitrate and phosphate from water, *International Journal of Biological Macromolecules*, 154, (2020), 188-197 https://doi.org/10.1016/j.ijbiomac.2020.03.074

[11] Christos Christou, Katerina Philippou, Theodora Krasia-Christoforou, Ioannis Pashalidis, Uranium adsorption by polyvinylpyrrolidone/chitosan blended nanofibers, *Carbohydrate Polymers*, 219, (2019), 298-305 https://doi.org/10.1016/j.carbpol.2019.05.041

[12] Y. Gao, P. Jiang, D. F. Liu, H. J. Yuan, X. Q. Yan, Z. P. Zhou, J. X. Wang, L. Song, L. F. Liu, W. Y. Zhou, G. Wang, C. Y. Wang, S. S. Xie, J. M. Zhang, D. Y. Shen, Evidence for the Monolayer Assembly of Poly(vinylpyrrolidone) on the Surfaces of Silver Nanowires, *The Journal of Physical Chemistry B*, 108, 34, (2004), 12877-12881 http://doi.org/10.1021/jp037116c

[13] Ritesh Kumar, Indrani Mishra, Gulshan Kumar, Synthesis and Evaluation of Mechanical Property of Chitosan/PVP Blend Through Nanoindentation-A Nanoscale Study, *Journal of Polymers and the Environment*, 29, 11, (2021), 3770-3778 https://doi.org/10.1007/s10924-021-02143-0

[14] Łukasz Wujcicki, Joanna Kluczka, Recovery of Phosphate(V) Ions from Water and Wastewater Using Chitosan-Based Sorbents Modified—A Literature Review, *International Journal of Molecular Sciences*, 24, 15, (2023), 12060 https://doi.org/10.3390/ijms241512060

[15] Umi Fathanah, Mirna Rahmah Lubis, Zuhra Mahyuddin, Syawaliah Muchtar, Mukramah Yusuf, Cut Meurah Rosnelly, Sri Mulyati, Rina Hazliani, Devi Rahmanda, Suraiya Kamaruzzaman, Meuthia Busthan, Sintesis, Karakterisasi dan Kinerja Membran Hidrofobik Menggunakan Polyvinyl Pyrrolidone (PVP) sebagai Aditif, *ALCHEMY Jurnal Penelitian Kimia*, 17, 2, (2021), 140-150 http://doi.org/10.20961/alchemy.17.2.48435.140-150

[16] C. S. Ong, W. J. Lau, P. S. Goh, B. C. Ng, A. F. Ismail, Preparation and characterization of PVDF–PVP–$TiO_2$ composite hollow fiber membranes for oily wastewater treatment using submerged membrane system, *Desalination and Water Treatment*, 53, 5, (2015), 1213-1223 https://doi.org/10.1080/19443994.2013.855679

[17] A. K. Wardani, D. Ariono, S. Subagjo, I. G. Wenten, Fouling tendency of PDA/PVP surface modified PP membrane, *Surfaces and Interfaces*, 19, (2020), 100464 https://doi.org/10.1016/j.surfin.2020.100464

[18] David Aili, Mikkel Rykær Kraglund, Joe Tavacoli, Christodoulos Chatzichristodoulou, Jens Oluf Jensen, Polysulfone-polyvinylpyrrolidone blend membranes as electrolytes in alkaline water electrolysis, *Journal of Membrane Science*, 598, (2020), 117674 https://doi.org/10.1016/j.memsci.2019.117674

[19] Xiaorui Ren, Huanhuan Li, Ke Liu, Hongyi Lu, Jingshuai Yang, Ronghuan He, Preparation and Investigation of Reinforced PVP Blend Membranes for High Temperature Polymer Electrolyte Membranes, *Fibers and Polymers*, 19, 12, (2018), 2449-2457 http://doi.org/10.1007/s12221-018-8361-2

[20] M. O. Mavukkandy, M. R. Bilad, J. Kujawa, S. Al-Gharabli, H. A. Arafat, On the effect of fumed silica particles on the structure, properties and application of PVDF membranes, *Separation and Purification Technology*, 187, (2017), 365-373 https://doi.org/10.1016/j.seppur.2017.06.077